NANO LETTERS

2007
Vol. 7, No. 4
1081−1085

An Efficient Bicomponent TiO_2/SnO_2 Nanofiber Photocatalyst Fabricated by Electrospinning with a Side-by-Side Dual Spinneret Method

Zhaoyang Liu,*,† Darren Delai Sun,*,† Peng Guo,‡ and James O. Leckie§

School of Civil and Environmental Engineering, Nanyang Technological University, Singapore 639798, Institute of Chemistry, Chinese Academy of Sciences, Beijing 100080, P R China, and Department of Civil and Environmental Engineering, Stanford University, Stanford, California 94305-4020

Received August 12, 2006; Revised Manuscript Received September 18, 2006

ABSTRACT

In this communication, we demonstrate that the electrospinning process with a side-by-side dual spinneret can be a simple approach for fabricating bicomponent TiO_2/SnO_2 nanofibers with controllable heterojunctions. Specifically, both of the TiO_2 and SnO_2 components in the nanofibers are fully exposed to the surface. This morphology fully utilized the photogenerated holes and electrons during the photocatalytic process, thus leading to a high photocatalytic activity. We believe that this versatile approach can be extended to fabricate other novel high-efficiency bicomponent photocatalysts.

Titanium dioxide (TiO_2) has been a popular photocatalyst for the treatment of organic pollutants in water and air.[1a,b] However, TiO_2 photocatalysts have an inherent and significant drawback; that is, the photogenerated charge carriers (hole−electron pairs) can recombine.[2] Therefore, to increase the photocatalytic activity of TiO_2, it is important to decrease the recombination of photogenerated charge carriers. Coupling TiO_2 with other semiconductors can provide a beneficial solution for this drawback.[3a−d] In a double-layered TiO_2/SnO_2 heterostructured film, according to the energy-level diagram (scheme SI 1, Supporting Information), the photogenerated electrons in the TiO_2/SnO_2 system accumulate on the SnO_2 and holes accumulate on the TiO_2 because of the heterojunction formed at the TiO_2/SnO_2 interface, which can result in a high quantum efficiency and high photocatalytic activity.[3a] However, if this kind of double-layered TiO_2/SnO_2 film was used as a photocatalyst, then there is a problem that the photogenerated electrons accumulated in the SnO_2 underlayer, which may be unavailable for participating in the photocatalytic reactions.[1b] During the process of photocatalytic reactions, the photogenerated holes are considered to directly oxidize organic pollutants, whereas the photogenerated electrons are shown to be capable of contributing to the oxidization process through the reduction of adsorbed O_2 to the superoxide radical ion, $^{\bullet}O_2^-$, which can take part in the oxidation process.[1b] Hence, as an ideal coupled photocatalyst, the two components should be fully exposed to the surface, which allows both photogenerated holes and electrons to take part in the photocatalytic reaction. Cao et al.[4] reported that a double-layered TiO_2/SnO_2 film was synthesized by a plasma-enhanced chemical vapor deposition (PECVD) technique, and they claimed that both of the two components could be exposed to the surface. However, their photocatalytic activity still depended on the extent of coverage of the SnO_2 underlayer by the TiO_2 overlayer. In addition, immobilized-film photocatalysts usually suffer a significant loss in surface areas, which limits their photocacalytic efficiency.[5] Recently, Chen et al.[6] reported that a coupled TiO_2/SnO_2 particle photocatalyst could be prepared by ball milling and showed an increased photocatalytic activity. However, they did not illustrate whether the two components were fully exposed to the surface. Moreover, the particle photocatalyst itself might repollute the treated water and air because of the tremendous difficulties in recovery. The particle photocatalyst might also show lower photocatalytic efficiency because of aggregation problems.[7] Therefore, the development of a new type of nanostructured photocatalyst with efficient electron−hole utilization (thus, high quantum efficiency), high surface area, and favorable recycling characteristics is a challenge for practical applications.

* Corresponding authors. E-mail: liu_zhaoyang2003@yahoo.com (Z.L.); DDSun@ntu.edu.sg (D.D.S.).
† Nanyang Technological University.
‡ Chinese Academy of Sciences.
§ Stanford University.

10.1021/nl061898e CCC: $37.00
Published on Web 09/29/2006

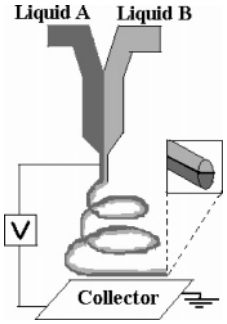

Figure 1. Schematic diagram of the experimental setup used for electrospinning bicomponent nanofibers with side-by-side dual spinnerets. When exposed to an applied electric potential, the two jetting liquids simultaneously experience an electrical field that is formed between the tips of the liquids and the counter-electrode (collector).

Electrospinning is a simple and versatile method for generating ultrathin fibers made of various materials under the influence of an electrostatic field.[8a−e] The diameter of the electrospun nanofibers could be conveniently controlled in the range of less than tens of nanometers, which is still a big challenge for other methods. The conventional setup for electrospinning uses a single capillary as the spinneret, which is only suitable for generating fibers with one particular composition.[9] Recently, a dual syringe system (in the side-by-side fashion) has been developed to electrospin biphasic Janus particles and bicomponent polymer nanofibers.[10a−c]

In this communication, we designed a new kind of bicomponent nanofiber photocatalyst consisting of TiO_2 and SnO_2 semiconductors. The nanofiber photocatalyst was fabricated by a simple electrospinning procedure with a side-by-side dual spinneret method. The advantages of the present bicomponent nanofibers are the following: (1) maximum exposure of both of the two components to the surface, which drastically reduces the recombination of the hole−electron pairs in the bicomponent system, thus increasing the quantum efficiency;[1b] (2) high surface areas,[11] which allows increased adsorption of various reactants and products during the photcatalytic reaction; and (3) favorable morphology for recovery and recycling.[12] Therefore, the resulting bicomponent nanofiber may be an attractive photocatalyst in environmental applications.

The experimental setup for bicomponent electrospinning was similar to that used for single-component electrospinning,[9] except for the configuration of the syringe setup, through which two distinct solutions were jetted simultaneously by using a dual-spinneret assembly. The dual syringes were confined in a side-by-side geometry (Figure 1). In a typical electrospinning process, the spinneret containing SnO_2 precursor solution had an inner diameter of 0.4 mm, whereas the other spinneret containing TiO_2 precursor solution had an inner diameter of 0.7 mm. Detailed properties of the precursor solutions are included in the Supporting Information. A distance of 14 cm and voltage of 14 kV were maintained between the tip of the spinneret and the collector. After electrospinning, these nanofibers were calcined in air at 500 °C for 2 h.

The morphology and structure of the products were characterized by X-ray diffraction (XRD, Rigaku DMAX/rC) with Cu KR radiation, and field emission scanning electron microscopy (FE-SEM, LEO1530) equipped with energy dispersion spectroscopy (EDS). X-ray photoelectron spectroscopy (XPS) experiments were carried out on a PHI 5000 instrument with an Al KR anode. Photoluminescence (PL) was measured at room temperature with a Hitachi luminescence spectrometer (F-4500) using a Xenon discharge lamp as the excitation light source, and the excited wavelength was 300 nm. SPS measurements were carried out with a solid-junction photovoltaic cell of indium tin oxide (ITO)/sample/ITO using a light source-monochromator-lock-indetection technique. Monochromatic light was obtained by passing light from a 500 W xenon lamp through a double-prism monochromator (Hilger and Watts, D300). A lock-in amplifier (Brookdeal, 9503-SC), synchronized with a light chopper, was employed to amplify the photovoltage signal. All experiments were carried out at room temperature.

The photocatalytic degradation of Rhodamine B (RhB) was carried out to demonstrate the photocatalytic activity. The aqueous system containing RhB (5.0×10^{-5} M, 100 mL) and photocatalyst (20 mg) was magnetically stirred in the dark for 30 min to reach the adsorption equilibrium of RhB with the photocatalyst and then exposed to UV light from a Upland Mineralight lamp (254 nm, 40 μw cm^{-2}). UV−vis absorption spectra of samples were recorded at different intervals to monitor the reaction. Total organic carbon (TOC) was measured by a Tekmar Dohrmann Apollo 9000 TOC analyzer.

The typical SEM images of the bicomponent TiO_2/SnO_2 nanofiber photocatalyst after being calcined at 500 °C are shown in Figure 2a and b. Like other single-component fibers prepared by electrospinning,[9] the bicomponent nanofibers were continuous and formed an unweaved mesh (Figure 2a). The average diameter of the bicomponent nanofibers was about 100 nm, and the length of them was in the range of centimeters. The higher-magnification SEM image (Figure 2b) indicates that the single fiber exhibited a bundle-like structure with two small nanofibers bound together. A distinct boundary is visible between the two small nanofibers, which indicates that the two parallel jetting solutions were fused together to form one single fiber during the electrospinning process. The diameter of each individual small nanofiber was ~50 nm. Chemical analysis of the small nanofibers using EDS is shown in Figure 2c. From the EDS results, it was shown that one of the two small nanofibers corresponded to SnO_2, and the other to TiO_2. This configuration of the bicomponent nanofiber ensured that both TiO_2 and SnO_2 were fully exposed to the surface. XRD results of the bicomponent TiO_2/SnO_2 and pure TiO_2 nanofibers calcined at 500 °C are shown in Figure 2d. In curve a of Figure 2d, it is shown that all diffraction peaks of the pure TiO_2 nanofibers could be perfectly indexed to the anatase TiO_2 phase (JCPDS file No. 21-1272). Whereas in curve b of Figure 2d, apart from the TiO_2 anatase peaks, there were some rutile SnO_2 peaks (JCPDS file No. 77-0450). Hence, it can be deduced that, in the bicomponent TiO_2/SnO_2

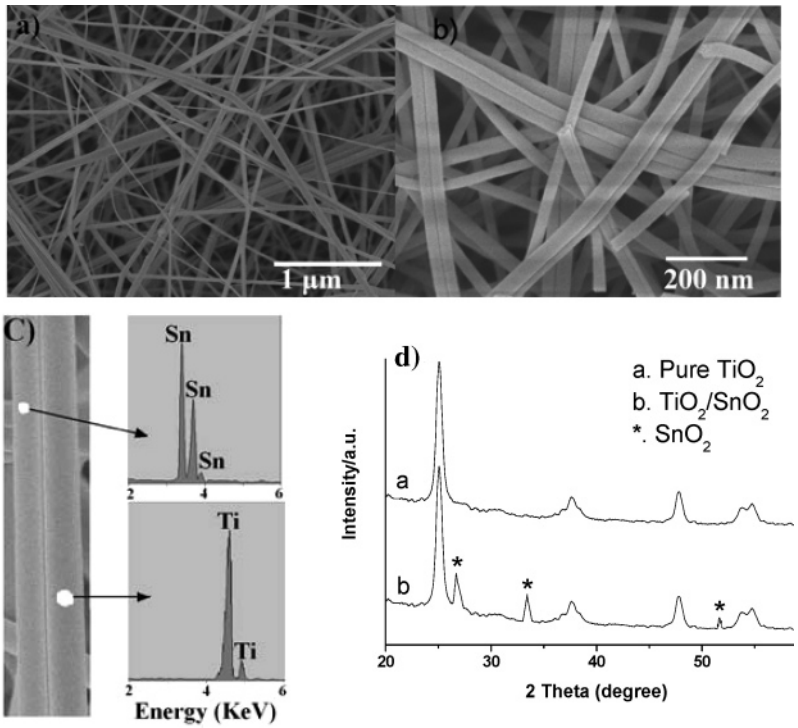

Figure 2. (a and b) Typical SEM images of the electrospun bicomponent TiO_2/SnO_2 nanofibers that were calcined at 500 °C; (c) Typical EDS microanalysis on selected areas of a single nanofiber, showing that the single nanofiber was indeed composed of two small TiO_2 and SnO_2 nanofibers that were bound together; (d) Typical XRD diffraction patterns of the electrospun nanofibers that were calcined at 500 °C for 2 h (the peaks labeled with asterisks correspond to the rutile phase of SnO_2 and all of the other peaks correspond to the anatase phase of TiO_2).

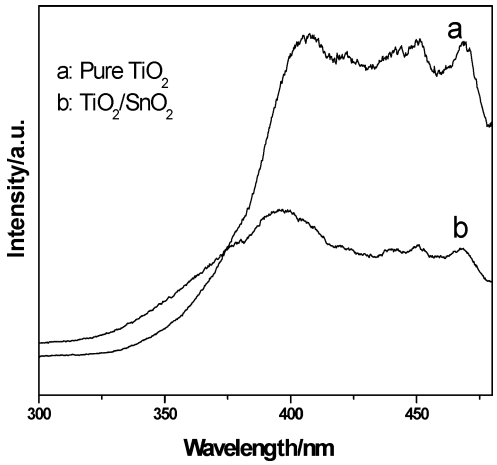

Figure 3. PL spectra of the electrospun bicomponent TiO_2/SnO_2 and pure TiO_2 nanofibers that were calcined at 500 °C.

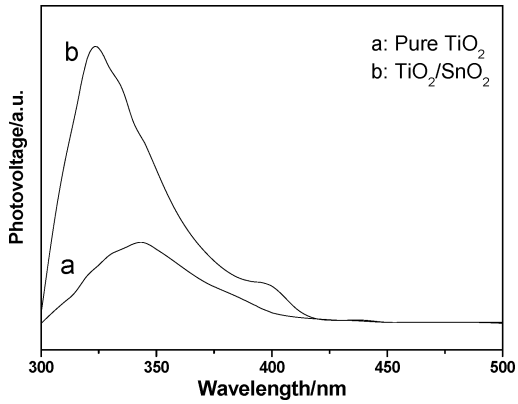

Figure 4. SPS of the electrospun bicomponent TiO_2/SnO_2 and pure TiO_2 nanofibers that were calcined at 500 °C.

nanofibers, the anatase TiO_2 phase and rutile SnO_2 phase coexisted. In addition, the XRD peaks of TiO_2 in the bicomponent TiO_2/SnO_2 nanofibers did not shift compared with the pure TiO_2 nanofibers. This indicates that the Sn element did not substitute into the TiO_2 lattices for Ti, and there was also no solid solution formation. The surface compositions and chemical states of the bicomponent TiO_2/SnO_2 nanofibers calcined at 500 °C were analyzed using XPS. Figure SI 2 (Supporting Information) shows the XPS spectra of Ti 2p and Sn 3d. The XPS peak positions of Ti $2p_3$ and Sn $3d_5$ were at about 458.5 and 486.4 eV, respectively, demonstrating that the main chemical states of Ti and Sn in the samples were both +4 valence.

The PL spectra is related to the transfer behavior of the photoinduced electrons and holes so that it can reflect the separation and recombination of photoinduced charge carriers.[13] Figure 3 shows the PL spectra of pure TiO_2 and bicomponent TiO_2/SnO_2 nanofibers calcined at 500 °C. It can be seen that the pure TiO_2 and bicomponent TiO_2/SnO_2 nanofibers both exhibited obvious PL signals upon irradiation with 300 nm light. Coupling SnO_2 had a great effect on the PL intensity of the TiO_2 nanofibers; the PL intensity decreased dramatically when the TiO_2 was coupled with the SnO_2. On the basis of these findings, it was concluded that

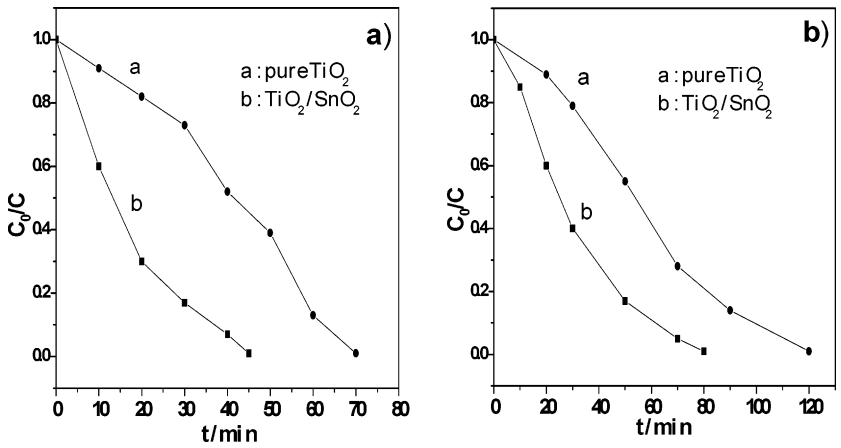

Figure 5. (a) Concentration changes of RhB dye and (b) TOC changes as a function of irradiation time under UV light with different nanofiber photocatalysts.

coupling SnO_2 results in the formation of heterojunctions between the small TiO_2 and SnO_2 nanofibers. The potential difference between TiO_2 and SnO_2 allowed photoelectrons to easily migrate from the TiO_2 surfaces to the SnO_2 conduction band. This resulted in a decrease in the radiation combination of photoinduced electrons on the TiO_2 surfaces, and further weaking the PL signal. Thus, the decreased PL intensity indicates a high quantum efficiency and possibly a high photocatalytic activity.

The SPS method is also a well-established technique for the characterization of semiconductors, mainly reflecting the carrier separation and transfer behavior with the aid of light.[4,13] It is well known that the higher the SPS signal, the higher the separation rate of photoinduced charge carriers. Thus, the photocatalytic properties of materials can be predicted primarily by the SPS method. The SPS responses of the bicomponent TiO_2/SnO_2 and pure TiO_2 nanofibers are shown in Figure 4. The bicomponent TiO_2/SnO_2 nanofibers exhibited a stronger SPS response than the pure TiO_2 nanofibers. This means that the separation rate of photoinduced electron−hole pairs was improved, suggesting that a high photoactivity can be expected in the bicomponent TiO_2/SnO_2 nanofibers. This result is in agreement with the above PL result.

The photocatalytic activities of the pure TiO_2 and bicomponent TiO_2/SnO_2 nanofibers were evaluated by the photocatalytic oxidation of RhB dye under UV light. Significant degradation and mineralization of RhB dye was observed (Figure 5a and b). As expected from PL and SPS measurements, the bicomponent TiO_2/SnO_2 sample exhibited a much higher photocatalytic activity than pure TiO_2. The linear correlation between ln C_0/C and t suggested a first-order reaction for all of the samples. The photocatalytic degradation rate of RhB dye on the bicomponent TiO_2/SnO_2 nanofibers was 0.089 min^{-1}, which was more than two times of that on the pure TiO_2 nanofibers (0.042 min^{-1}).

The current fabrication method is simple and straightforward, and consequently can be used to produce other coupled semiconductor photocatalysts. For example, we fabricated a bicomponent nanofiber photocatalyst from TiO_2 and V_2O_5 precursors using a similar fabrication method. Typical SEM and EDS (as shown in Figure SI 3 of the Supporting Information) show that the single bicomponent TiO_2/V_2O_5 nanofiber photocatalyst was composed of individual TiO_2 and V_2O_5 small nanofibers, similar to the bicomponent TiO_2/SnO_2 nanofibers. Similarly, the fabricated bicomponent TiO_2/V_2O_5 nanofiber photocatalyst showed higher photocatalytic activity than pure TiO_2 nanofiber photocatalyst.

In conclusion, a novel-structure nanofiber photocatalyst consisting of two components, TiO_2 and SnO_2, has been prepared by a simple electrospinning process with a side-by-side dual spinneret method. The morphologies of the electrospun bicomponent nanofibers made it possible for both of the TiO_2 and SnO_2 components to be fully exposed at the surface. This special heterojunction structure could promote an increase in the charge separation of the photogenerated electrons and holes within the bicomponent system, allowing both of the photogenerated electrons and holes to participate in the overall photocatalytic reaction. The bicomponent TiO_2/SnO_2 nanofiber was demonstrated to be an excellent photocatalyst. We believe that the electrospinning method described in this manuscript can be extended easily to prepare a new generation of high-efficiency photocatalysts from a wide variety of coupled materials. For example, we were able to fabricate a bicomponent TiO_2/V_2O_5 nanofiber photocatalyst using a similar fabrication procedure.

Supporting Information Available: Energy-level diagram and XPS spectra of TiO_2/SnO_2 nanofibers, figures showing TiO_2/V_2O_5 nanofibers and details on nanofiber precursors. This material is available free of charge via the Internet at http://pubs.acs.org.

References

(1) (a) Linsebigler, A. L.; Lu, G.; Yates, J. T., Jr. *Chem. Rev.* **1995**, *95*, 735. (b) Hoffmann, M. R.; Martin, S. T.; Choi, W.; Bahnemann, D. W. *Chem. Rev.* **1995**, *95*, 69.

(2) Honda, H.; Ishizaki, A.; Soma, R.; Hashimoto, K.; Fujishima, A. *J. Illum. Eng. Soc.* **1998**, *27*, 42.

(3) (a) Levy, B.; Liu, W.; Gilbert, S. *J. Phys. Chem. B* **1997**, *101*, 1810. (b) Kutty, T. R. N.; Avudaithai, M. *Chem. Phys. Lett.* **1989**, *163*, 93. (c) Serpone, N.; Maruthamuthu, P.; Pichat, P. *J. Photochem. Photobiol., A* **1995**, *85*, 247. (d) Liu, Z.; Quan, X.; Fu, H.; Li, X.; Yang, K. *Appl. Catal., B* **2004**, *52*, 33

(4) Cao, Y.; Zhang, X.; Yang, W.; Hui, D.; Bai, Y.; Li, T.; Yao, J. *Chem. Mater*. **2000,** *12*, 3445.
(5) Shephard, G. S.; Stochenstrom, S.; Villiers, D. d.; Engelbrech, W. J.; Wessels, G. F. S. *Water Res.* **2002**, *36*, 140
(6) Chen, S.; Chen, L.; Gao, S.; Cao, G. *Mater. Chem. Phys.* **2006**, *98*, 116.
(7) Rachel, A.; Subrahmanyam, M.; Boule, P. *Appl. Catal., B* **2002**, *37*, 301.
(8) (a) Norris, D.; Shaker, M. M.; Ko, F.; MacDiarmid, A. G. *Synth. Met.* **2000**, *114*, 109. (b) Reneker, D. H.; Chun, I. *Nanotechnology* **1996**, *7*, 216. (c) Dietzel, J. M.; Kleinmeyer, J.; Harris, D.; Beck Tan, N. C. *Polymer* **2000**, *42*, 261. (d) Bognitzki, M.; Czado, W.; Frese, T.; Schaper, A.; Hellwig, M.; Steinhart, M.; Greiner, A.; Wendroff, J. H. *Adv. Mater.* **2001,** *13*, 70. (e) Fong, H.; Chun, I.; Reneker, D. H. *Polymer* **1999,** *40*, 4585.
(9) Li, D.; Xia, Y. *Nano Lett.* **2003**, *3*, 555
(10) (a) Roh, K.; Martin D.; Lahann, J. *Nat. Mater.* **2005**, *4*, 759. (b) Gupta, P.; Wilkes, G. L. *Polymer* **2003**, *44*, 6353. (c) Madhugiri, S.; Dalton, A.; Gutierrez, J.; Ferraris, J. P.; Balkus, K. J., Jr. *J. Am. Chem. Soc.* **2003**, *125*, 14531.
(11) McCann, J. T.; Marquez M.; Xia Y., *J. Am. Chem. Soc.* **2006**, *128*, 1436.
(12) Zhan, S.; Chen, D.; Jiao, X.; Tao, C. *J. Phys. Chem. B* **2006**, *110*, 11199
(13) Jing, L.; Fu, H.; Wang, B.; Wang, D.; Xin, B.; Li, S.; Sun, J. *Appl. Catal. B: Environ.* **2006**, *62*, 282.

NL061898E